Journal of Engineering Physics and Thermophysics, Vol. 73, No. 2, 2000

MATHEMATICAL SIMULATION OF THE TEMPERATURE FIELD IN HARDENING GEARS BY INDUCTION HEATING UNDER A LAYER OF WATER

P. S. Gurchenko and M. L. German

UDC 621.891:621.793

We consider a mathematical model of heat exchange in strainless successive high-frequency-current hardening of the working surfaces of gears. The dynamics of the process of heating and cooling is analyzed, its special features are indicated, and the advantages of the technology of hardening gear tooths by this technique are considered.

Introduction. A technology of strainless contour hardening of the toothed surface of gears in induction heating under a layer of running water has been developed, introduced into production, and used at the Minsk Automobile Plant and the Minsk Plant of Wheeled Tractors [1, 2]. The technique suggested is distinguished by absence of thermal strains, high rates of heating (up to 10,000 °C/sec) and cooling (to 6000 °C/sec), high hardness of the surface treated (58–62 HRC for steels containing 0.38–0.45% carbon), economic efficiency, and environmental safety. Metallographic and x-ray examinations of gears hardened according to this technology were carried out in [3-5]. Below we consider problems of numerical calculation of the thermokinetic parameters of heating and cooling a layer of the toothed surface of gears subjected to induction hardening.

Determination of the Thermokinetic Parameters of Hardening. A schematic representation of induction hardening of a toothed surface is given in Fig. 1. The hardening begins with rapid heating of a narrow 3–5-mm-wide strip along the upper edge of the lateral surface of a tooth over the entire length treated. The inductor wire moves continuously relative to the hardened toothed surface from the tooth point to the tooth space and then to the point of a neighboring tooth, successively traversing its surface from point 1 to point 7 (Fig. 1). The entire cycle of hardening from the first to the last tooth proceeds automatically and then the machine tool trips open. The total hardening time for the entire surface of one tooth space is 1.5–3 sec, and the hardening time for the entire gear is 3–6 min.

The treated toothed surface of the gear is heated according to the considered technology at a rate attaining 10,000 °C/sec under a layer of running water, with the gap between the inductor and the heated surface being 0.3–0.6 mm. Under these conditions direct measurements of temperature are virtually unfeasible by available methods. In this connection it is of interest to calculate the heating temperature and the heating and cooling rate by the method of mathematical computer simulation of the process of induction hardening of a toothed surface. In calculations, the rate and electrical parameters of heating and the thermophysical and electrical properties of the steels used and the cooling medium were taken into account.

The mathematical model for determining the temperature fields in a material subjected to high-frequency currents is based on solution of the well-known Fourier heat-conduction equation, which in the presence of internal heat sources has the form [6]

$$c_p(T)\,\rho(T)\,\frac{\partial T(\vec{r},\tau)}{\partial \tau} + \nabla\left(-\lambda(T)\,\nabla T(\vec{r},\tau)\right) = Q_v(\vec{r},\tau)\,. \qquad (1)$$

Academic Scientific Complex "A. V. Luikov Heat and Mass Transfer Institute," National Academy of Sciences of Belarus, Minsk, Belarus; "Minsk Automobile Plant" Industrial Association, Minsk, Belarus. Translated from Inzhenerno-Fizicheskii Zhurnal, Vol. 73, No. 2, pp. 423-429, March–April, 2000. Original article subnitted October 21, 1998.

 1062-0125/00/7302-0420$25.00

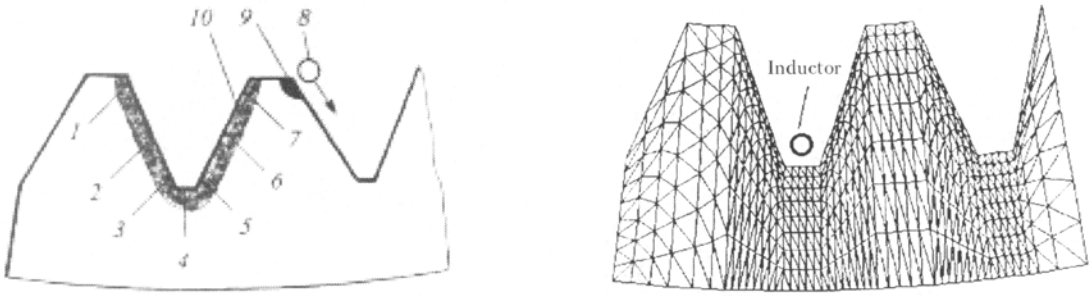

Fig. 1. Position of control points 1-7, the inductor 8, an elementary hot zone in the process of hardening 9, and the calculated hardened layer 10 in the cross section of the toothed surface of a gear of the wheel transmission of an MAZ truck.

Fig. 2. Spatial discretization of a gear fragment.

The boundary conditions for Eq. (1) that allow for convective and radiative mechanisms of heat transfer from the body surface can be written in the form

$$-\lambda(T)\frac{\partial T(\vec{r},\tau)}{\partial \vec{n}} = \alpha(T)\left(T(\vec{r},\tau) - T_{en}\right) + \varepsilon\sigma\left(T^4(\vec{r},\tau) - T_{en}^4\right). \tag{2}$$

At the initial instant ($\tau = 0$) we assign the temperature distribution in the body:

$$T(\vec{r},\tau)\big|_{\tau=0} = T_0. \tag{3}$$

The temperature of a piece is determined by solving heat-conduction equation (1) with boundary conditions (2) and initial conditions (3). The indicated system is solved by the finite-elements method [7]. According to this method, spatial discretization of the computational domain is carried out (Fig. 2), which yields a certain number of elements of division (N_e) and nodal points (N_p) at which the temperature is calculated. For each i-th nodal point ($1 \le i \le N_p$) the basis functions $\psi_i(\vec{r})$ are introduced in such a way that $\psi_i(\vec{r_i}) = 1$ and $\psi_i(\vec{r_j}) = 0$, $\forall\, j \ne i$, where $1 \le l \le N_p$, i.e., the function ψ_i represents a hyperpyramid constructed above the i-th nodal point. Then the temperature $T(\vec{r},\tau)$ can be expressed in terms of the basis functions in the following way:

$$T(\vec{r},\tau) = \sum_{j=1}^{N_p} T_j(\tau)\,\psi_j(\vec{r}). \tag{4}$$

To determine T_j, we use the Bubnov–Galerkin method, in conformity with which for each $1 \le i \le N_p$ Eq. (1) yields

$$\iiint_W \left(c_p(T)\,\rho(T)\frac{\partial T(\vec{r},\tau)}{\partial \tau} + \nabla\left(-\lambda(T)\,\nabla T(\vec{r},\tau)\right) - Q_v(\vec{r},\tau) \right) \psi_i(\vec{r})\, dw = 0, \tag{5}$$

where $W = \bigcup_{e=1}^{N_e} \Delta_e$ is the computational domain; Δ_e is the e-th element of division.

With account for Eq. (4), Eqs. (5) are reduced to the system of linear equations

$$\sum_{j=1}^{N_p} \frac{\partial T_j(\tau)}{\partial \tau} \sum_{e=1}^{N_e} \iiint_{\Delta_e} \left(c_p(T)\,\rho(T)\,\psi_i(\vec{r})\,\psi_j(\vec{r})\right) dw +$$

$$+\sum_{j=1}^{N_p} T_j(\tau) \sum_{e=1}^{N_e} \left(\iiint_{\Delta_e} \lambda(T)\, \nabla\psi_i(\vec{r})\, \nabla\psi_j(\vec{r})\, dw + \iint_{\delta\Delta_e} \psi_i(\vec{r})\, \psi_j(\vec{r})\, \tilde{\alpha}(T)\, ds \right) =$$

$$= \sum_{e=1}^{N_e} \iiint_{\Delta_e} Q_v(\vec{r},\tau)\, \psi_i(\vec{r})\, dw + \sum_{e=1}^{N_e} \iint_{\delta\Delta_e} \psi_i(\vec{r})\, \tilde{q}(T)\, ds\,, \tag{6}$$

where the quantities $\tilde{\alpha}(T)$ and $\tilde{q}(T)$, with account for boundary conditions (2), are defined as follows:

$$\tilde{\alpha}(T) = \alpha(T) + \varepsilon\sigma\,(T^3 + T_{en}^2 + TT_{en}^2 + T_{en}^3)\,,\quad \tilde{q}(T,\tau) = \tilde{\alpha}(T,\tau)\, T_{en}\,. \tag{7}$$

Here $\delta\Delta_e$ is the face of the e-th element belonging to the surface of the piece.

For further consideration it is convenient to write the system of equations (6) in matrix form:

$$\mathbf{M}^c(\tau) \cdot \frac{\partial \mathbf{T}(\tau)}{\partial\tau} + \mathbf{M}^\lambda(\tau) \cdot \mathbf{T}(\tau) = \mathbf{Y}(\tau)\,, \tag{8}$$

where $\mathbf{Y}(\tau)$ and $\mathbf{T}(\tau)$ are the vectors of the values on the right-hand side of system (8) and the temperature at the nodal points of the computational grid; the superscripts λ and c indicate, respectively, the thermal conductivity and heat capacity coefficients that determine the matrix. Equation (8) is solved by the Crank–Nicolson difference scheme [8]:

$$\hat{\mathbf{M}}^c(\tau) \cdot \frac{\mathbf{T}(\tau^{k+1}) - \mathbf{T}(\tau^k)}{\Delta\tau} + \frac{1}{2}\hat{\mathbf{M}}^\lambda(\tau) \cdot (\mathbf{T}(\tau^{k+1}) + \mathbf{T}(\tau^k)) = \hat{\mathbf{Y}}(\tau)\,, \tag{9}$$

where $\Delta\tau = \tau^{k+1} - \tau^k$ is the time step. With account for Eq. (9), we can write an expression to determine $T(\tau^{k+1})$:

$$\mathbf{T}(\tau^{k+1}) = (\mathbf{M}_\tau)^{-1} \cdot [\mathbf{M}_0 \cdot \mathbf{T}(\tau^k) + \mathbf{Y}_0]\,, \tag{10}$$

where

$$\mathbf{M}_\tau = \hat{\mathbf{M}}^c - \frac{\Delta\tau}{2}\hat{\mathbf{M}}^\lambda,\quad \mathbf{M}_0 = \hat{\mathbf{M}}^c + \frac{\Delta\tau}{2}\hat{\mathbf{M}}^\lambda,\quad \mathbf{Y}_0 = \Delta\tau\hat{\mathbf{Y}}\,.$$

Taking into account the fact that the resulting matrices $\mathbf{M}_\tau$ and $\mathbf{M}_0$ are band-type and positive definite, it is convenient to invert the matrix $\mathbf{M}_\tau$ in expression (10) by Kholesskii's method [8], which requires less computer resources for storing and solving the matrices.

With allowance for the above the algorithm for calculation of the temperature fields $T(\vec{r},\tau)$ can be represented in the following way:

1) the initial distribution of temperature $T_0(\vec{r})$ is prescribed, $\tau = 0$;

2) the next instant $\tau^{k+1} = \tau^k + \Delta\tau$ is determined;

3) the volumetric density of the internal heat sources $Q_v(\vec{r},\tau)$ at the nodal points of the computational grid and the coefficients $\tilde{\alpha}(T)$ and $\tilde{q}(T)$ are determined;

4) according to the above-described method of solving the heat-conduction equation (1) and in accordance with Eq. (6) the matrices $\mathbf{M}_\tau$ and $\mathbf{M}_0$ and the vector of the right-hand side $\mathbf{Y}(\tau)$ are filled and then, in accordance with Eq. (10), the temperatures at the nodal points $T_i(\tau^{k+1})$ of the computational grid are calculated;

5) if the computational time is smaller than the prescribed one, the calculation is repeated from item 2.

Determination of the Volumetric Density of the Internal Heat Sources. The volumetric density of the internal heat sources is defined by the expression [9]

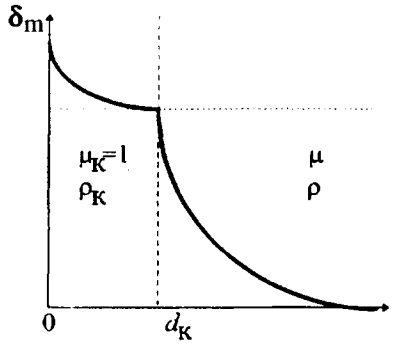

Fig. 3. Distribution of the current density over the cross section of the heated material.

$$Q_v(\vec{r},\tau) = \frac{1}{2}\rho(T(\vec{r}))\,\delta_m^2(\vec{r},\tau), \tag{11}$$

where ρ is the specific electrical resistance of the heated material, Ω·m. The density of the current within the material depends on the surface density of the current $\delta_{m.s}$:

$$\delta_m(\vec{r},\tau) = \delta_{m.s}(\tau)\exp(-d(\vec{r})/\Delta), \tag{12}$$

$$\Delta \approx 503\sqrt{\left(\frac{\rho}{\mu f}\right)} \tag{13}$$

is the depth of current penetration, m. By virtue of the fact that μ and ρ are functions of temperature, in what follows, according to the method of calculation of inductors [9], the quantity Δ will be understood to mean the *effective* depth of penetration of the current:

$$\Delta \approx \frac{\Delta_K}{\sqrt{2}\,K\cos\varphi}, \tag{14}$$

where $\Delta_K \approx 503\sqrt{\rho_K/f}$ is the depth of current penetration into the material heated above the temperature of magnetic transformations ($T_K \approx 750°C$), the so-called "hot" penetration depth.

In accordance with the indicated method, we consider a two-layer material: one layer of thickness d_K is heated above T_K, and the temperature of the other layer is lower (Fig. 3). According to this method, the coefficient K entering Eq. (14) and the angle φ are defined by the following expressions [9]:

$$m = (1-\sqrt{\rho_K\mu/\mu_K\rho})/(1+\sqrt{\rho_K\mu/\mu_K\rho});$$

$$\tan\left(\varphi-\frac{\pi}{4}\right) = \frac{2m\exp(-\alpha)\sin(\alpha)}{1-m^2\exp(-2\alpha)},\quad \alpha = 2d_K/\Delta_K; \tag{15}$$

$$K = \frac{\sqrt{(1-m^2\exp(-2\alpha))^2 + 4m^2\exp(-2\alpha)\sin^2(\alpha)}}{1+m^2\exp(-2\alpha)+2m\exp(-\alpha)\cos(\alpha)}.$$

The current density on the surface of the heated piece is calculated proceeding from the current strength in the inductor, the effective penetration depth of the current, and the equivalent width of the heated strip (Fig. 4):

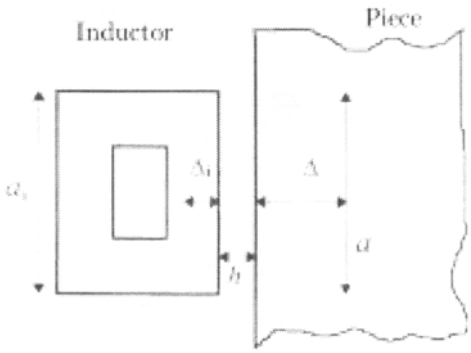

Fig. 4. Schematic diagram for calculating the electrical resistance of the system.

$$\delta_{m.s} = \frac{I_i}{a\Delta}. \tag{16}$$

The current strength in the inductor is determined in terms of the generator power and the resistance of the inductor-piece system:

$$I_i^2 = \eta P/z, \tag{17}$$

where η is a correction factor that takes into account the losses in the electrical circuit before the inductor.

The resistance of the inductor-piece system is

$$z = \sqrt{(r_i + r)^2 + (x_i + x + x_g)^2}, \tag{18}$$

where x_g is the reactive resistance determined by the magnetic flux in the air gap. The electrical resistance of an inductor that has w closely wound turns is

$$r_i \approx x_i \approx w \frac{\pi D_i}{b} \frac{\rho_i}{\Delta_i} = w^2 \frac{\pi D_i}{a} \frac{\rho_i}{\Delta_i}, \tag{19}$$

where D_i is the equivalent inside diameter of the inductor; $b = a/w$ is the width of a turn of the inductor in the case of close winding. The electrical resistance of the piece is

$$r \approx x \approx \frac{\pi D \rho}{a\Delta} \tag{20}$$

(D is the equivalent diameter of the piece). The reactive resistance of the air gap is

$$x_g \approx 2\pi f \mu_0 w^2 \frac{S_h}{a}, \tag{21}$$

where $\mu_0 \approx 4\pi \cdot 10^{-7}$ H/m is the magnetic permeability of vacuum; $S_h = Lh$ is the cross-sectional area of the air gap, m^2 (L is the inductor length, h is the gap (Fig. 4) between the piece and the inductor). For a cylindrical inductor we have $S_h = \pi(D_i + D)h/2$.

Taking into account the aforesaid, the expression for the volumetric density of the internal heat sources in the case of inductive heating can be written in the following form:

$$Q_v(\vec{r}, t) = \eta\rho \frac{P(\tau)}{2z(a\Delta)^2} \exp(-2d(\vec{r})/\Delta), \tag{22}$$

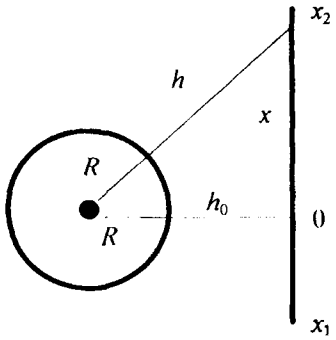

Fig. 5. Calculation of the equivalent heated strip for an inductor with a circular cross section.

In expression (22) all the quantities are defined by the above formulas, except for the equivalent width of the strip heated. According to the method of calculation of inductors [9], for rectangular inductors (Fig. 4) the width of this strip is taken to be equal to the width of the inductor, i.e., $a \approx a_i$.

For an inductor with a circular cross section of the wire no recommendations are given. In view of this, to determine the equivalent heated strip a model is suggested that is based on the assumption that

$$\delta_{m.s} = \delta_{m0} (h_0/h)^2 . \tag{23}$$

Then the magnitude of the equivalent heated strip is determined from the condition of equality of heated cross sections (Fig. 5):

$$a = \int_{x_1}^{x_2} \left(\frac{h_0}{h(x)} \right)^2 dx , \tag{24}$$

$$h(x) = \sqrt{(R + h_0)^2 + x^2} - R , \tag{25}$$

where R is the radius of the cross section of the induction wire; x_1 and x_2 are the coordinates of the beginning and the end of the heated piece with account taken of the fact that the coordinate origin lies directly under the inductor (Fig. 5).

When an inductor with a circular cross section heats more than one side of a piece (see Fig. 2), the volumetric density of heat generation is calculated separately for each side proceeding from the fact that there are several heating strips connected in parallel. Then the total electrical resistance of the inductor-piece system is

$$z = 1 \Big/ \sum_{i=1}^{n} 1/z_i , \tag{26}$$

where z_i is the electrical resistance of the system consisting of the i-th strip being heated and the corresponding strip on the inductor. For the current density on the surface of the i-th strip the following expressions can be obtained:

$$(\delta_m^i)^2 = \eta \frac{Pz}{z_i^2 (a_i \Delta_i)^2} \left(\frac{h_{min}}{h_i} \right)^4 , \tag{27}$$

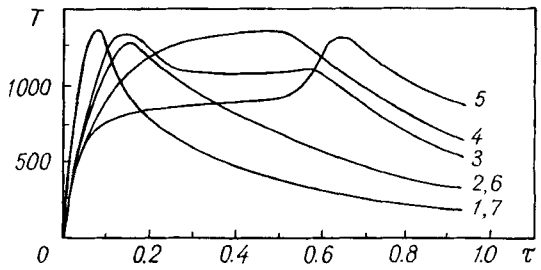

Fig. 6. Thermal curves of heating and cooling at control points 1-7, constructed computationally for the process of induction hardening of the toothed surface of a gear of the wheel transmission of an MAZ truck. Conditions of hardening: generator power 160 kW, speed of inductor motion over the middle part of the involute 15 mm/sec, inducting-wire diameter 2.6 mm, gap between the inducting wire and the treated surface 0.5 mm. T, °C; τ, sec.

where a_i is the equivalent strip being heated on the i-th side undergoing heating; h_i is the gap between the inductor and the piece on the i-th side being heated; h_{min} is the minimum inductor-piece gap over all the surfaces being heated.

Considering what has been said above, the expression for the volumetric density of the internal heat sources on the i-th heated side in induction heating can be written in the form

$$Q_v^i(\vec{r},\tau) = \eta\rho_i \frac{P(\tau)\, z}{2z_i (a_i \Delta_i)^2} \left(\frac{h_{min}}{h_i}\right)^4 \exp(-2d(\vec{r})/\Delta_i) . \tag{28}$$

The devised program of mathematical simulation of induction heating and cooling of the toothed surface of gears allows one to carry out a theoretical construction of thermal curves of heating and cooling for any point of the surface and core of the gear treated. Figure 6 shows thermal curves of heating for hardening and cooling calculated by the method of computer simulation for each of the seven control points of the toothed surface (see Fig. 1).

The differences in the shape of the thermal curves for different zones and stages of heating agree with the physical foundations of induction heating and correspond to the hardening results obtained. At the tip the induction current is concentrated on a narrow edge, the heat removal into the interior of the piece is smallest, and therefore both during entry of the inductor into the tooth space (Fig. 1, point 1) and during exit from it (point 7) the heating rate is greatest.

Of interest is the character of the thermal curves for points 3, 4, and 5. When the inductor approaches point 3, the surface of the tooth in this zone is first heated rapidly, and then the heating decreases as a result of loss of magnetic properties by the surface layers of the metal and uptake of part of the power by the approached surface. Simultaneously with the continuing heating of zone 3 heating of zone 4 in the tooth space and zone 5 of the opposite lateral surface of the tooth begins. In view of the simultaneous removal of power by zones 3, 4, and 5 and also of the fact that the removal of heat into the boundary parts of the metal is greatest for zone 4, the heating rate at this point is considerably lower than for points 1, 2, 6, and 7. Since the inductor is close to point 3, the temperature in it in this period is maintained virtually constant for some time. As the inductor leaves the tooth space, the stage of cooling begins simultaneously at points 3 and 4.

For point 5 heating begins at a time when heating for points 3 and 4 still continues. Therefore in the initial period the heating rate in it is relatively reduced. After the inductor recedes from points 3 and 4, the energy emitted by the inductor is concentrated in zone 5, and the heating rate in it increases sharply. When the inductor recedes from this point, the stage of cooling begins in it.

Thus, the calculated rate of heating of the treated surface at the tooth tips for zones 1 and 7 attains 10,000 °C/sec and in the space (point 4) it attains 5000 °C/sec. The temperature of surface heating attains 1100–1400°C. The calculated rate of cooling of the surface being hardened is 1000–6000 °C/sec. The calculated data agree well with the values actually obtained for the depth of hardening, evaluated by the hardness and structure of the hardened zone in the process of metallographic examinations. The theoretical position of the layer of surface hardening shown in Fig. 1 agrees with the actually obtained position of the hardened layer over the cross section of the toothed surface of gears.

Conclusion. Mathematical simulation of induction heating of the toothed surface of gears makes it possible to determine the dependence of the thickness and the character of disposition of the hardened layer on the treated surface on the parameters of the inductor and the high-frequency source used and the geometric dimensions and the grade of steel of the gear treated. Mathematical prediction of the results of hardening reduces labor and time expenditures when selecting high-frequency sources, technological parameters of hardening, and the structure of hardening devices.

NOTATION

$T(\vec{r},\tau)$, temperature of the body at the radius vector $\vec{r}$ at time τ, °C; c_p, ρ, and λ, heat capacity, density, and thermal conductivity of the material of the body, J/(kg·K), kg/m^3, W/(m·K), respectively; $Q_v(\vec{r},\tau)$, volumetric density of the internal heat sources due to absorption of electromagnetic energy, W/m^3; $\vec{n}$, external normal to the surface of the piece; ε, emissivity of the surface; $\sigma \approx 5.67 \cdot 10^{-8}$ W/(m^2·K^4), Stefan–Boltzmann constant; α, coefficient of heat transfer from the piece into the surrounding medium, W/(m^2·C); δ, current density in the material, A/m^2; d, distance from the point having the radius vector $\vec{r}$ to the surface of the piece; μ, relative magnetic permeability of the material; f, current frequency in the inductor, Hz; I, strength of the current, A; a, equivalent width of the heated strip, m; P, power of the generator, W; z, electrical resistance of the inductor-piece system, Ω; r and x, active and reactive electrical resistance, respectively, Ω. Subscripts: en, environment; p, nodal point; e, element of the discretization; s, surface of the piece; m, material of the piece; i, inductor. The sign ^ indicates the mean value of some quantity during a certain interval of time.

REFERENCES

1. P. S. Gurchenko, V. M. Bykov, and Yu. I. Shumakov, *A Technique for Inductive Hardening of Gears and an Inductor Used for That Purpose*, Patent of the Republic of Belarus No. 209 (1993).
2. P. S. Gurchenko and N. S. Karpushkin, *A Lathe for Continuous-Successive Hardening of Gears*, Patent of the Republic of Belarus No. 1838 (1997).
3. P. S. Gurchenko, in: *Kola Zebate KZ-96, Miedzunarodowa Konferencja Naukowo-Technizna, Materialy Konferencji*, Poznan (1996), pp. 73-80.
4. P. S. Gurchenko and G. G. Panich, in: *Kola Zebate KZ-96, Miedzunarodowa Konferencja Naukowo-Technizna, Materialy Konferencji*, Poznan (1996), pp. 80-85.
5. P. S. Gurchenko, *Vestsi Nats. Akad. Navuk, Ser. Fiz.-Tékh. Navuk*, No. 3, 66-75 (1998).
6. V. P. Isachenko, V. A. Osipova, and A. S. Sukomel, *Heat Transfer*, 4th rev. and augm. edn. [in Russian], Moscow (1981).
7. O. Zenkevich, *Method of Finite Elements in Engineering* [Russian translation], Moscow (1975).
8. J. Crank and P. Nicolson, *Proc. Cambridge Philos. Soc.*, No. 43, 7-19 (1947).
9. A. E. Slukhotskii and S. E. Ryskin, *Inductors for Inductive Heating* [in Russian], Leningrad (1974).